Coronal origins of the solar wind - sources of steady streams and transient flows caused by solar magnetic eruptions

E. Marsch

Max-Planck-Institut für Sonnensystemforschung, 37191 Katlenburg-Lindau, Germany

Abstract. The magnetic field of the Sun and the plasma properties of its atmosphere, such as temperature distribution, density stratification, photospheric convection and waves in the corona, determine the origin, energetics and evolution of the solar wind. The solar wind comes in three main kinds, as steady fast streams, variable slow flows and transient slow and fast coronal mass ejections. The three types of solar wind are closely associated with the structure and activity of the coronal magnetic field. The plasma characteristics and magnetic features of the solar wind source regions are reviewed. The boundary conditions in the mostly closed corona (streamers and loops), in the transiently opening corona (eruptive prominences and loops) and in the lastingly open corona (funnels and holes) will be analyzed. The resulting properties of the solar wind are discussed.

Index Terms. Origin of solar wind, solar magnetic field, solar wind types, coronal mass ejections.

1. Introduction

The solar wind is basically determined by the Sun's magnetic field and responds in various ways to solar activity and the accompanying changes in the photospheric magnetic field, which determines the coronal magnetic field and therewith the interplanetary magnetic field and solar-wind stream structure in the entire heliosphere. For a modern review of the solar magnetic field see Solanki et al. (2006). The sources of the solar wind are defined by the field, and the origin of the solar wind is closely linked with and influenced by the activity in the magnetic network.

As the result of varying boundary conditions in the corona, three basic types of solar wind occur: Fast streams from large coronal holes (CHs); slow streams from small CHs and active regions (ARs), and from the boundary layers of coronal streamers; and the variable transient flows such as coronal mass ejections (CMEs), often associated with eruptive prominences, or plasmoids stemming from the top of streamers, and other ejections from ARs driven through magnetic reconnection. These basic types of solar wind are closely associated with the structure and the activity of the coronal magnetic field (for recent reviews see, e.g., Marsch, 2006, and Schwenn, 2006) that changes over the solar cycle.

This paper gives a concise review of the origin of the solar wind, with emphasis on the magnetic nature of the source regions, as they become evident in the solar extreme ultraviolet (EUV) emission patterns and in coronagraph images. The plasma characteristics as well as the magnetic structures of the solar wind source regions are reviewed. The boundary conditions in the mostly closed corona (streamers and loops), in the transiently opening corona (eruptive prominences and loops) and in the lastingly open corona (funnels and holes) will be analyzed, in particular at small scales, and discussed from the observational point of view.

2. Dynamic magnetic network

The Sun's magnetic field together with the plasma properties and processes in its lower atmosphere, such as photospheric convection, temperature distribution, density stratification, current sheets and plasma waves, largely determine the origin and evolution of the solar wind.

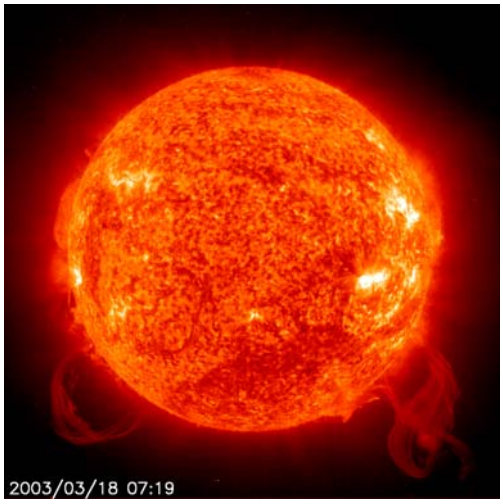

Fig. 1. Magnetic network and prominences as seen in the emission line of helium at a wavelength of 30.4 nm, which forms at about 60000-80000 K and thus depicts relatively cool material in the lower corona. Prominences often are at the origin of coronal mass ejections. The network is the location at which waves are believed to be generated by reconnection between small loops, a process enforced by magnetoconvection, and where current sheets may form, the dissipation of which will lead to coronal heating. The image is courtesy of the team of EIT on SOHO.

The magnetic network is shown in Fig.1. It appears to be at the origin of the steady, fast and slow, solar wind streams and seems to harbor the energy source for the heating of the open solar corona and the acceleration of the solar wind. The activity of the network field is most likely responsible for these processes, as was suggested long ago by Porter and Moore (1987) and amply described by Parker (1991, 1992). The overall activity of the magnetic carpet, the dynamics of ephemeral regions and their consequences for coronal heating are discussed by Schrijver et al. (1999). Multiple small loops (at a scale of one megameter or smaller) will owing to magnetoconvection approach each other and collide, and may by merging constitute a prolific source of energy, perhaps also associated with high-frequency waves (Axford and McKenzie, 1997) which will ultimately dissipate in the funnels of the lower corona (Marsch and Tu, 1997).

3. Solar wind and coronal magnetic field

Before continuing with the discussion of the global coronal magnetic field, we will address some basic energetics and typical parameters of the solar wind. The required energy flux density at 1 R_S is $F_E = 5\ 10^5$ erg cm^{-2} s^{-1} to drive the fast solar wind, the terminal speed beyond 10 R_S observationally is V_p = 700 - 800 km s^{-1}, the remotely inferred temperatures at 1.1 R_s are $T_e \approx T_p \approx$ 1-2 10^6 K, and the in-situ measured values at 1 AU are $T_p = 3\ 10^5$ K, $T_\alpha = 10^6$ K, and $T_e = 1.5\ 10^5$ K. For heavy ions the temperature ratio scales in proportion to their mass ratio, i.e., $T_i \cong m_i / m_p\ T_p$, with the ion differential speed obeying the relation $\mathbf{V_i - V_p = V_A}$, phenomena that are still asking for an explanation. For more details on the fluid and kinetic properties of the interplanetary solar wind plasma see the review paper of Marsch (1991).

The energy requirement on the solar wind can be estimated from the Bernoulli-type energy equation, which compares the coronal enthalpy with the sum of the gravitational binding energy and asymptotic kinetic energy of a solar wind proton,

$$\gamma/(\gamma-1)2k_BT_C=1/2m_p(V_\infty^2+V_p^2). \quad (1)$$

Here the polytropic index is γ=5/3, and the escape speed from the solar surface is V_∞ = 618 km s^{-1}. The effective coronal temperature T_C must be about 10^7 K, in order to obtain a wind flow speed of V_p = 700 km s^{-1} in Earth orbit. This temperature is by an order of magnitude higher than typical values in the open corona, and therefore the related energy comes most likely from waves. The fluxes of energy and mass must be somehow generated in, or continuously fed through, the magnetic network and brought to the corona. The total energy required to sustain the fast solar wind corresponds for a proton-electron pair to a specific value of about 5 keV. For a more comprehensive discussion of solar wind models and theory see the reviews by Axford and McKenzie (1997) or Marsch et al. (2003), who also address aspects of kinetic solar wind theory and observations.

The coronal magnetic field has hardly ever been measured directly, but it can be obtained by force-free extrapolation techniques (for a summary of the state of the art in this field see, e.g., Wiegelmann and Neukirch, 2002). An example of the resulting model field of the active Sun is shown in Fig. 2, after Wiegelmann and Solanki (2004). Clearly, an active region mainly consists of closed magnetic loops, in which dense plasma is confined, and which therefore cause bright emission. In contrast, the large-scale magnetic field is open in CHs, from which tenuous plasma can escape on open field lines as solar wind, and where the emission is strongly reduced as a result. This fact is obvious in any of the ultraviolet EIT images, which regularly are obtained on SOHO and therefore not reproduced here again.

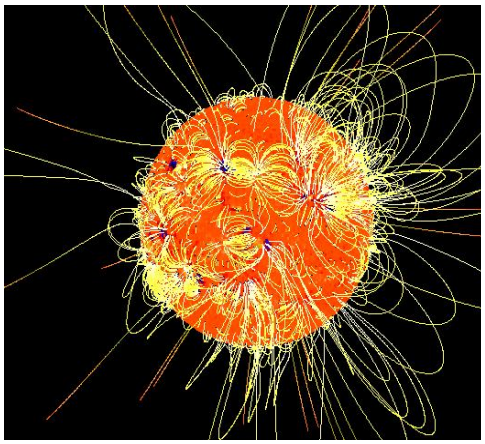

Fig. 2. Coronal magnetic field as obtained by force-free extrapolation from photospheric magnetograms after Wiegelmann and Solanki (2004). The closed loops mostly correspond to bipolar active regions, or also may bridge widely separated regions of opposite polarity, whereas the open lines illustrate the coronal magnetic field that is open to the heliosphere and corresponds to the magnetic flux carried away by the solar wind.

The solar magnetic field determines the solar wind flow pattern and the structure of the corona. The coronal magnetic field gradually evolves with increasing distance from the Sun into the heliospheric (interplanetary) magnetic field. At some height, corresponding to the so-called source surface which is usually assumed to be located at 2.5 to 3 R_S, the field becomes frozen into the solar wind.

The source surface is a virtual sphere from which on the outer coronal field is assumed to be radial. The potential-field model extrapolates the field measured in the photosphere to the corona, while postulating that the whole coronal field is free of currents. Thus the polarity changes only across the heliospheric current sheet (HCS), which is linked with the equatorial streamer belt, and during solar minimum extends as a symmetric disk far out into interplanetary space. Hoeksema (1995) has described this model, and in particular the solar magnetic field and HCS as they evolved during the early Ulysses epoch over a full solar cycle. Marsch (2006) reviewed solar-wind responses to the Sun's magnetic

activity.

The structure of the solar corona is simplest around minimum activity, where the field can be well modeled by a superposition of dipolar, quadrupolar, and current-sheet-related components after Banaszkiewicz et al. (2000). This minimum-type corona is shown in Fig. 3. The related three-dimensional structure of the solar wind was only fully revealed by the Ulysses mission. In a grand overview plot, McComas et al. (2003) have illustrated the global structure of the solar wind and its variation over the solar cycle. Over the poles, high-speed solar wind originating in the polar CHs prevails in solar minimum, whereas slow wind coming from the streamer belt then dominates at low latitudes. The magnetic field becomes multipolar towards solar maximum activity, and the solar wind source regions accordingly change in locations and spatial extents. Similarly, the solar wind flow pattern becomes more complex and variable.

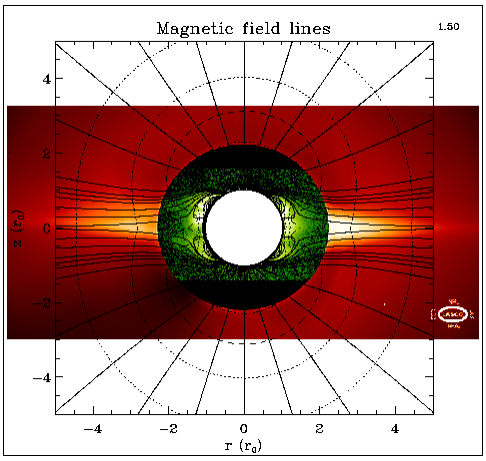

Fig. 3. The highly symmetric solar corona at minimum activity (after Forsyth and Marsch, 2000) and the associated magnetic field according to the model of Banazkiewicz et al. (2000). Superposed coronal images from EIT and LASCO (green corona line) indicate the large polar CH and the low-latitude current sheet coinciding with the streamer belt.

The changing solar corona and associated wind are shown in Fig. 4, which reproduces the general survey plot after McComas et al. (2000) and gives a sequence of coronal images in the top panel and the solar wind speed in the bottom panel versus time and heliographic latitude. The transition from the minimum-type corona around 1995 to a maximum-type near 1999 is obvious and accompanied with a striking transition from steady fast to variable slow solar wind. The recurrent-stream oscillations between 1996 and 1997 are due to solar rotation that causes rapid transitions of the spacecraft into and out of the HCS, respectively the open field related to the polar CHs, and thus results in a periodic variation between fast and slow flows. At the bottom, the occurrence times of CMEs are also indicated, which tend to accumulate around maximum solar activity when the corona is highly structured magnetically and of multi-polar nature.

The other, as compared to a steady stream, basic type of (variable and sporadic) solar wind (or better storm) is a coronal mass ejection. For CMEs the energy requirements and acceleration mechanisms are understood much worse than for the steady streams. We will discuss CMEs in more detail in the subsequent sections. The recent review by Zhang and Low (2005) emphasizes the hydromagnetic nature of CMEs, and it provides a list of the relevant theoretical literature and gives a summary of the basic theory and model ideas. The energy constraints are even tougher for a transient CME than for a steady solar wind stream, as its plasma density is often much higher and its flow speed may easily reach a multiple of the average solar-wind speed.

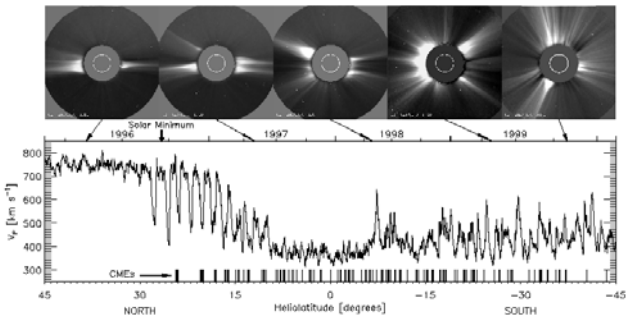

Fig. 4. The changes of the solar corona (top) over the solar cycle and the corresponding variations in the solar wind flow pattern (after McComas et al., 2000) as a function of time or heliographic latitude along the Ulysses spacecraft orbit. Note the recurrent streams after mimum. The occurrence of CMEs is marked by the small vertical bars attached to the bottom scale.

4. Coronal mass ejections and magnetic flux eruptions

At times, the solar atmosphere is strongly disturbed by flares, magnetic flux eruptions, and by CMEs that are perhaps the most spectacular processes in the solar corona, and certainly the most relevant for space weather. When hitting the Earth, they may have a strong impact in particular on the near-Earth plasma environment (Schwenn et al., 2005), and they often trigger or cause magnetospheric storms that are again associated with auroras. A nice example of a CME is given in Fig. 5, which is a composite of an EIT image and a LASCO coronagraph image from SOHO.

Some statistics may be of interest here. The frequency of CME occurrence is about 3 events per day in solar maximum and 0.3 events per day in solar minimum (Webb and Howard, 1994). The mass is estimated to range between 5 1012 kg and 5 1013 kg. Often, CMEs attain the shape of so-called magnetic clouds in the interplanetary space (Bothmer and Schwenn., 1998). The velocities may widely vary and can range from 20 km s-1 to 2500 km s-1, and the travel time to Earth also varies a lot, from many hours up to several days, with typically 80 hours. CMEs reveal variable shapes and have complex magnetic field configurations, which are discussed in more detail below. A comprehensive review of their properties before the SOHO era was given by Hundhausen (1999), and for the past ten years of space observations from SOHO the characteristics of CMEs were reviewed by St.Cyr et al. (2004).

There are two basic types of CMEs which can be discriminated according to their initial acceleration or velocity-versus-height profile in the solar corona. So-called fast CMEs are flare-associated and start with very high initial speed of typically 700 kms^{-1} or even more, but show low acceleration with a = 0.3 m s^{-2}, whereas the slow CMEs are associated with solar eruptive events and start at very low initial speed of 10-20 kms^{-1}, but have a high acceleration with a = 5-50 m s^{-2}. These so-called balloon-type CMEs still accelerate more rapidly than the quasi-steady slow solar wind originating from the tip of the coronal streamer belt (Sheeley et al, 1997). The speed-versus-height profile of slow CMEs after Srivastava et al. (1999) is shown in Fig. 6. The radial profiles flatten off beyond 10-15 R_S, where the acceleration gradually ceases. Often a CME reveals a complex fine structure and consist of three main components, an outer bright loop corresponding to a magnetic flux tube, then inside of it a dark void, and finally an innermost bright kernel.

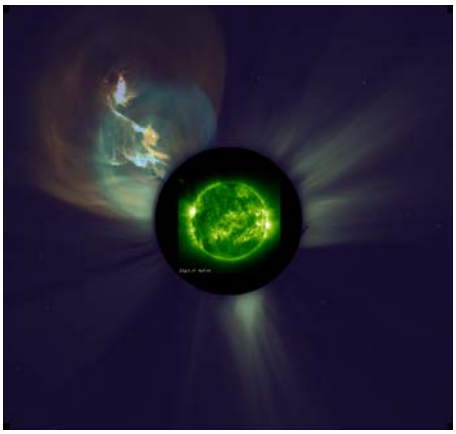

Fig. 5. Coronal mass ejection as seen by SOHO with the C2 coronagraph of LASCO (two images superposed). The insert shows a standard disk image taken by the EIT instrument. Some coronal streamers are also seen at the bottom and on the top right side. Note the bubble-shaped CME with its nested shells and its narrow and dense (brighter) filamentary core part, which reveals a kind of winding pattern (courtesy Cremades and Bothmer, 2005).

The physical processes leading to the strong acceleration are not fully understood (for a recent review of the models and different theories see Zhang and Low, 2004), but they are certainly of magnetohydrodynamic nature, and very likely involve an excessive Lorentz force, as it may arise from transient force imbalances in the coronal plasma, and which can be generated by surface magnetic activity through freshly emerging magnetic flux and by motions of the foot points of magnetic field lines rooted in the photosphere.

What are the sources of CMEs at the solar surface? As will be discussed below, an eruptive prominence often is at the origin of a CME. Two examples were already shown in the previous Fig. 1, where the ultraviolet emission off the solar limb reveals the prominence by its helical winding pattern. It is due to the field stresses and represents the magnetic helicity which was presumably accumulated in the coronal field by previous convective motions of the field lines while being anchored in the photosphere.

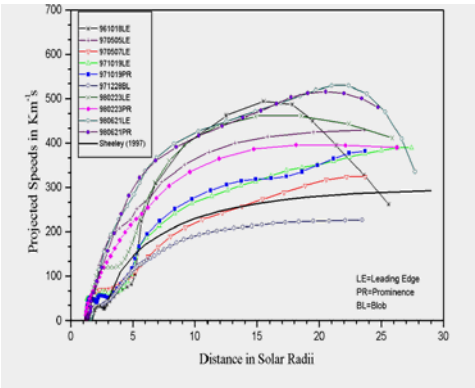

Fig. 6. Speed-versus-height profiles of different coronal mass ejections as observed on SOHO with the coronagraph LASCO. The black continuous line gives the average slow-wind profile as it was derived by means of small plasma blobs emanating at about 2 R_S from the top of the coronal streamer belt. The initial acceleration of a slow CME can be high and range from 5 to 25 km s^{-1} (after Srivastava et al, 1999).

5. Coronal origins and sources of CMEs

In the SOHO epoch, CMEs have become a central subject of solar research. For a short phenomenology of CMEs and their properties see for example the tutorial paper of Srivastava and Schwenn (2002). A concise review of the present understanding of CMEs was, with a look to the future given, by Linker et al. (2003), who discussed the different models of CMEs, originating for example from helmet streamer eruption triggered by coronal magnetic flux cancellation, or forming through streamer reformation accompanied by reconnection in the aftermath of the eruption. A large number of CMEs are in fact caused by filament (prominence) eruptions. Their interplanetary manifestations often take the shape of magnetic clouds, which have conserved the helicity of the original flux tube of the erupted prominence. That was shown by Bothmer and Schwenn (1998), who analysed the polarity and orientation of the filaments that created magnetic flux ropes and clouds in the interplanetary solar wind. Their results are summarized in Fig. 7, which shows the helicities of the original prominences together with the helicities of the resulting CMEs that have the shape of magnetic clouds.

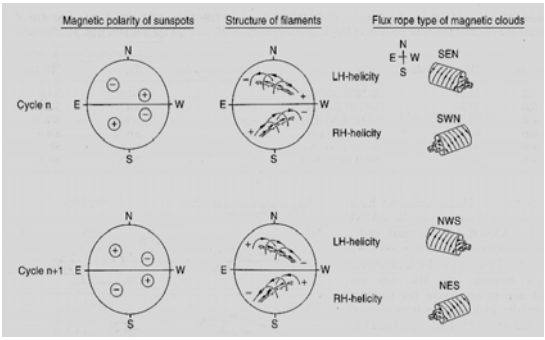

Fig. 7. Magnetic polarity of sunspots, magnetic winding structure of the filaments, and the helicities of the flux rope of the associated interplanetary magnetic clouds (after Bothmer and Schwenn, 1998).

Tripathi et al. (2004) studied the basic characteristics of EUV post-eruptive arcades (PEAs) and found that they are useful tracers of CME source regions on the Sun. A large set of PEAs fully visible on the disk were selected and correlated with SOHO/LASCO observations of whitle-light CMEs, with the intention to locate their source regions on synoptic magnetic charts. The PEAs were identified as reliable tracers of the CME source on the solar disk, and found to have positions matching the location of the active region belts in both solar hemispheres. The authors summarized the basic features of many PEAs observed over five years.

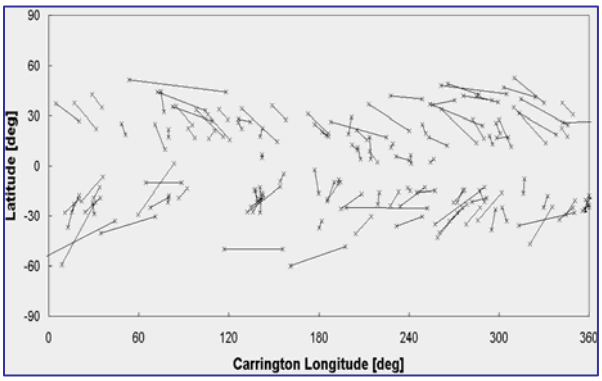

Fig. 8. Locations and extents of the identified source regions of CMEs, being associated with eruptive prominences, are displayed as a function of the solar latitude and longitude (after Cremades and Bothmer, 2004).

Cremades and Bothmer (2004) studied what they defined to be structured CMEs, which were found to arise from small-scale coronal loops. They existed prior to the CME eruption and were found to bridge bi-polar regions on the Sun. From the analysis of the magnetic structure of these source regions, the authors defined a generic scheme for the occurrence of a structured CME. The white-light appearance of a CME off limb in the LACSO coronagraph was found to depend primarily on the position and orientation of the neutral line of the associated bi-polar region on the Sun's disk. The results of their study are presented in Fig. 8, which shows the angular location and extent of the source regions.

Cremades and Bothmer (2004) also provided statistics of structured coronal mass ejections as observed by LASCO. The paper contains information about the white-light characteristics of the analyzed CMEs, for example angular width and position angle. They investigated the CME source region properties, such as heliographic location, inclination and length, including frequency and variation of these parameters over the investigated part of the solar cycle.

The study by Cremades and Bothmer (2004) showed that CMEs in three dimensions often attain an elongated shape with a preferred axis, which is given by the neutral line separating regions of opposite polarity in the CME source region on the Sun. This axis seems to correspond to the long axis of a large helical magnetic flux rope anchored on the Sun, with the prominence being the bottom part of this huge magnetic system. The orientation of the neutral line is often aligned with the prominence axis.

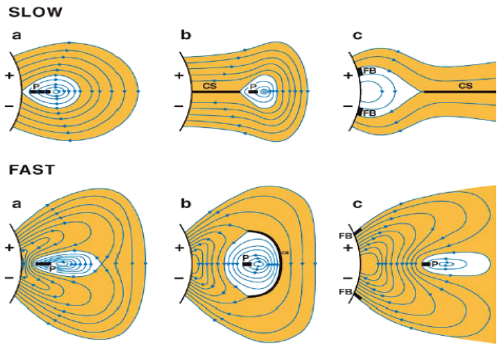

Fig. 9. The two basic scenarios proposed by Zhang and Low (2004) for the generation of CMEs. The two main types discussed in the text are shown. The slow (top) and fast (bottom) CME differ by the topology of the magnetic field in their source region and the location of the current sheet involved.

There is no standard paradigm for the CME origin yet. For a comprehensive review of the theories of CME initiation see Forbes (2000). A CME, while representing the coronal and interplanetary outcome of a magnetic flux rope originating in the low corona, will after lift-off suffer an enormous expansion in space, a process that is illustrated in Fig. 9 after Zhang and Low (2004). They considered the origin of CMEs from the theory point of view. Slow and fast CMEs considerably differ, which is mainly due to different magnetic field configurations and currents sheets involved, which are either assumed in the model or inferred from observations to exist above and below the erupting flux tube.

The CME expansion is most dramatic within the first few solar radii. Ultimately, the expanding coronal flux rope may be identified with a magnetic cloud in the solar wind (Bothmer and Schwenn, 1998). The true 3-D topology of a CME can only by established by means of multi-point observations. The future STEREO mission will, for the first time, provide such CME images taken from two different widely separated vantage points in the heliosphere.

6. Various source regions of the solar wind

Whereas the global association of fast wind with large CHs and of slow wind with the streamer belt and small CHs is long well established, the tracing of the in-situ observed solar wind to its detailed sources at smaller scales on the Sun is not an easy task. In this section we will present recent results in which the sources were identified through a combined analysis of Doppler shifts and radiances of ultraviolet emission lines together with the coronal magnetic field, as it was obtained by extrapolation from a magnetogram measured in the solar photosphere.

The steady solar wind consists of two major components: fast, tenuous, and uniform flows from large CHs, and slow,

dense, and variable flows from small CHs, often from near the boundaries between closed and open coronal fields. Riley et al. (2003) discussed various techniques of mapping such flows back to the Sun in order to identify their sources in the corona. Whereas the origin of fast streams seems clear, the slow wind sources remain less obvious. Recently, Arge et al. (2003) for example studied what appeared to be narrow CHs in the Yohkoh soft X-ray images, and identified them to be the sources of slow solar wind, which also revealed large magnetic-field expansion factors. Similarly, Ohmi et al. (2003) by using WIND spacecraft data found that slow streams can emanate from small CHs in the vicinity of ARs.

A. Solar wind from coronal funnels

The detailed source regions of the fast solar wind were recently found by Tu et al. (2005a) to be identical with the so-called coronal funnels in a CH, i.e. expanding magnetic field structures rooted in the magnetic network lanes. These authors corroborated and complemented the earlier work of Hassler et al. (1999), and established that the solar wind starts flowing out of the corona at heights above the photosphere between 5 Mm and 20 Mm in the funnels. This result was obtained by a correlation of the Doppler-velocity and radiance maps of different spectral lines. Specifically, Ne^{7+} ions were found to mostly radiate around 20 Mm, where they have outflow speeds of about 10 kms^{-1}, whereas C^{3+} ions with no average flow speed mainly radiate around 5 Mm. These new findings are illustrated in Fig. 10, which shows in two planes color-coded maps of the magnetic field strength at a height of 4 and 20 Mm. Regions with outflow speed larger than 7 km s^{-1} are indicated by the hatched patches that coincide with open unipolar field representing a funnel.

Stimulated by these observations, a new model was suggested to explain the origin of the fast solar wind. The transition region (TR) in CHs is full of magnetic loops of different sizes, mostly with a height of less than 5 Mm. The supergranular convection in the photosphere keeps the feet of the loops moving and thus transfers kinetic energy to magnetic energy that is stored in the loops. They may finally collide with the funnel and reconnect with pre-existing open fields. Thereby, plasma of the loops is released, which may lead to both upflows and downflows. Ultimately, parts of the plasma contained in reconnecting loops are brought into the corona. In the lower TR below about 5 Mm, we mainly have horizontal exchange of mass and energy between neighboring flux tubes, which is driven by supergranular motion. Above 5 Mm or higher, where reconnection between field lines of funnels and surrounding loops gradually ceases, vertical transport will become more important than horizontal, and the radial acceleration of the solar wind will actually start. This scenario (Tu et al., 2006) is illustrated in Fig. 11. It is a further development of the magnetic furnace idea of Axford and McKenzie (1997).

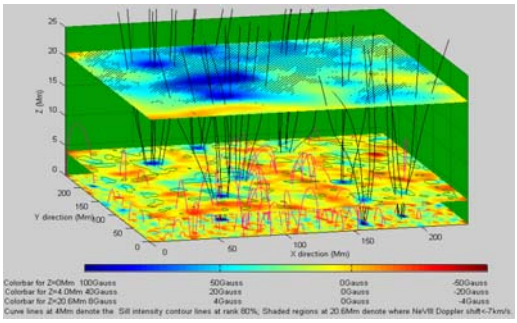

Fig. 10. Source regions of the fast solar wind in the magnetic funnels of a CH. The magnetic field magnitude is shown in two planes at 4 Mm and 20 Mm. The hatched areas indicate outflow speeds of neon ions larger than 7 km s^{-1}. The open field is indicated by black lines, and the closed loops in magenta color. They hardly reach a height of 10 Mm (after Tu et al., 2005a).

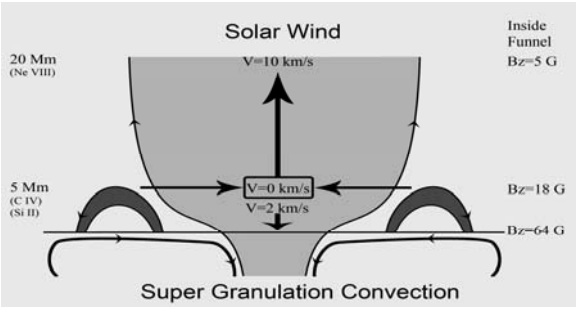

Fig. 11. Source regions of the fast solar wind in a magnetic funnel of a CH. This sketch illustrates the scenario of the solar wind origin and its energy and mass supply, mainly through side loops. Ultimately, convection is the driver of solar wind outflow in coronal funnels. Mass and also wave energy are delivered to the funnel by magnetic reconnection. Funnel and loops are drawn according to their real scale sizes (after Tu et al., 2006).

B. Solar wind from active regions

It is only recently, that ARs near solar maximum were clearly identified as the source regions of slow solar wind. For example, Liewer et al. (2003) investigated the magnetic topology of several ARs in connection with EUV and X-ray images. Synoptic coronal maps were employed for mapping the inferred sources of the solar wind from the magnetic source surface down to the photosphere. In most cases, a dark lane, as it is familiar for the small CHs, was seen in the EUV images, thus suggesting an open magnetic field. They studied in particular a magnetogram for AR 1934 and used a magnetic field extrapolation model, thus mapping the open flux from the source surface at 2.5 R_S to the photosphere. Thus several different sources (ARs and CHs) became clearly evident. They are shown in Fig. 12 which was taken from Liewer et al. (2003). In the synoptic map the arrows indicate the mapping of the solar wind from the source surface (arrow tails) to the photosphere (heads). The in-situ composition data of the solar wind associated with these regions indicates high freezing-in temperatures of the heavy ions, a result that is consistent with the inference that the AR indeed is a genuine source of the solar wind.

Marsch et al. (2004) also studied ARs in connection with coronal the magnetic field as obtained by extrapolation and together with EUV Doppler shifts and images. They

could establish that the dark (in ultraviolet emission) areas adjacent to the closed AR loops can indeed be magnetically open, and apparently reveal strong upflows in hot coronal emission lines. An example is given in Fig. 13, where on the left side the magnetic field of AR 7953 associated with a sunspot is shown, as obtained by force-free field extrapolation (see the review of Wiegelmann and Neukirch, 2002), and on the right side the Doppler-shift pattern indicating strong local plasma flows in the coronal loops of the AR. In the sunspot, the material clearly streams upward with a speed of several 10 km s^{-1}, whereas the adjacent closed loops are mostly related to downflows. Whether the upflow actually continues into the upper corona for this AR remains unclear, but it appears to be likely according to the results shown above in Fig. 12.

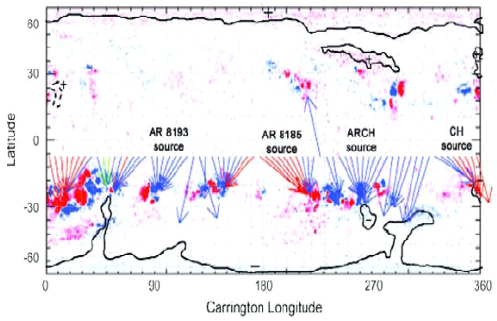

Fig. 12. Source regions of the solar wind, which is found to originate in active regions and small CHs. The arrows indicate the mapping of open flux from the source surface (at 2.5R_S) back to the photosphere. Red (blue) is inward (outward) magnetic polarity, and the green lines lie near the current sheet (after Liewer et al., 2003).

In conclusion, solar wind at times comes from the active Sun, i.e. ARs and their small neighbouring CHs. How many of such regions during solar maximum are associated with slow solar wind remains to be investigated. The question is still open if solar wind can also originate in the quiet corona, which consists of closed magnetic loops of different sizes.

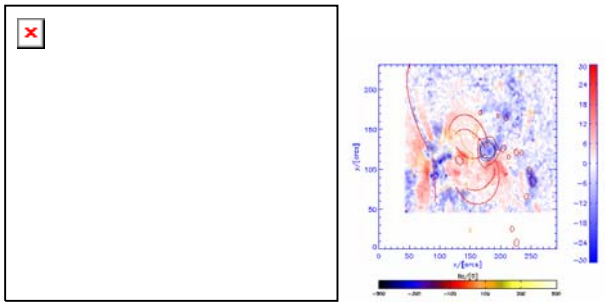

Fig. 13. *Left*: Coronal magnetic field topology in three dimensions for the bipolar AR 7953. Field lines above the solar surface with B_z > 50 G on the photosphere are plotted. The color coding represents the magnetic field strength. *Right*: SUMER Dopplergram in NeVIII (λ 77 nm) and a 2-D-projection of selected reconstructed field lines, as obtained from a force-free-field extrapolation with the model parameter α = -1.1 10^{-8} m^{-1}. Additional colored contours of the magnetic field strength on the photosphere are also shown. Note the sizable flows, reaching speeds of 25 km s^{-1}, with significant outflow in the sunspot at the center of the AR (after Marsch et al., 2004).

C. Solar wind from the quiet sun?

From correlations between the radiance of solar ultraviolet emission and the vertical magnetic field component, as obtained by extrapolation from photospheric magnetograms to different heights, one can determine the correlation height of the emission source, by identifying the altitude at which the correlation coefficient has its maximum. In this way Tu et al. (2005b) found that for a quiet-Sun region the correlation height for Si II is near 2.1 Mm, C IV at 1.4 Mm, and Ne VIII 3.7 at Mm. The thickness of the TR is thus determined to be only about 2 Mm. The height profiles are illustrated in Fig. 14, which also shows on the left the related magnetic-field map at 2.1 Mm, with superimposed contours of silicon-line radiances that coincide with regions of strong magnetic field.

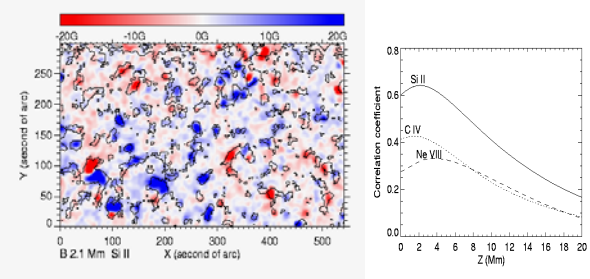

Fig. 14. *Left*: Magnetic field intensity color-coded with superimposed contours of the SiII radiance for a quiet-sun region of the lower solar corona. Note the clear correlation between field strength and line intensity. *Right*: Correlation heights defining the mean altitude of the emission region for three ultraviolet lines. The TR height is about 2 Mm (after Tu et al., 2005b).

A comparison between the extrapolated field lines and the Dopplershifts of Ne VIII indicates that weak blueshifts of 5 km s^{-1} occur in a few small regions with strong magnetic fields. Some of the closed field lines may reach as high as 10 Mm. Weak blueshifts do appear on both closed bi-polar regions and open unipolar regions. The low TR appears to be highly structured by a carpet of magnetic loops of different sizes. Most of the ultraviolet radiation is certainly coming from these loops. However, it remains unclear how much open magnetic flux exist in between the closed loops in the quiet corona, and how slow solar wind may originate there.

7. Discussion and summary

In this paper we reviewed the coronal origins of the solar wind and the sources of steady streams and transient flows. Obviously, the solar magnetic field is the main player in the relevant physical processes, since it shapes the solar corona and thus defines the properties and dynamics of the nascent solar wind. The magnetic field topology and activity are the keys to understand how the solar wind originates in the solar corona. Since the unsigned radial magnetic flux at 1 AU is measured to be almost constant over the full sphere and at any time, there must be a constant fraction of open magnetic magnetic flux in the lower corona at any time of the solar cycle. As the Sun's magnetic field varies systematically over the solar cycle, from a simple dipolar structure (in minimum)

to a complex multipolar structure (in maximum), so do the solar wind sources, and correspondingly varies the solar wind itself. Its plasma and energy have continuously to be supplied through the magnetic network into the TR and lower corona. Reconnection in the network appears to play a main role in the supply of mass and energy to the corona and solar wind.

The minimum-type slow wind, which can perhaps be modeled as a steady boundary layer flow (of a CH), for which the flux-tube expansion factor seems empirically to be connected with the terminal wind speed. The steady fast solar wind appears to originate in rapidly expanding funnels (unipolar) in CHs, and some slow wind may as well be generated in narrow unipolar open, or transiently open, funnels between myriads of dynamic loops in the quiet sun. Yet, there remain basic questions as to the origin of the slow wind. As measured in situ, it appears to be filamentary and intrinsically variable, a property that most likely reflects the time-variability of its coronal sources. In summary:

- The coronal magnetic field determines the origin and evolution of the solar wind at all scales.
- The solar wind comes in three types, as steady fast streams, variable slow flows and transient CMEs.
- The fast streams in minimum appear to originate in the funnels of polar coronal holes.
- The slow streams in minimum come from streamers and their boundaries, whereas in maximum they originate in small CHs and near ARs.
- CMEs seem to come in two main types, as slow and fast, although this classification is not unique.
- A sizable fraction of CMEs have large eruptive prominences at their origin, the remnants of which can be observed as post-eruptive arcades.

Acknowledgment. The author thanks the Deutsches Zentrum für Luft- und Raumfahrt (DLR) for travel support.

References

C. N. Arge, K. L. Harvey, H. S. Hudson and S. W. Kahler, in *Solar Wind Ten*, M. Velli, R. Bruno and F. Malara Eds. AIP Conf. Proc., vol. 679, Melville, NewYork, USA, 2003, p. 202.

W. I. Axford and J. F. McKenzie, in *Cosmic Winds and the Heliosphere*, J. R. Jokipii, C. P. Sonett and M. S. Giampapa Eds. Arizona University Press, Tucson, 1997, pp. 31-66.

M. Banaszkiewicz, W. I. Axford and J. F. McKenzie, *Astron. Astrophys.*, vol. 337, p. 940, 1998.

V. Bothmer and R. Schwenn, *Ann. Geophysicae*, vol. 16, p. 1, 1998.

H. Cremades and V. Bothmer, *Astron. Astrophys.* vol. 422, p. 307, 2004.

T. G. Forbes, *Geophys. Res.* vol. 105, p. 23153, 2000.

R. Forsyth and E. Marsch, *Space Sci. Rev.* vol. 89, p.7, 1999.

E. N. Parker, *Astrophys. J.* vol. 372, p. 719, 1991.

E. N. Parker, *J. Geophys. Res.* vol. 97, p. 311, 1992.

J. G. Porter, R. L. Moore, E. J. Reichmann, O. Engvold and K. L. Harvey, *Astrophys. J.*, vol. 323, p. 380, 1987.

D. A. Hassler *et al.*, *Science*, vol. 283, p. 810, 1999.

J. T. Hoeksema, *Space Sci. Rev.*, vol. 72, pp. 137-140, 1995.

A. J. Hundhausen, in *The many faces of the sun: a summary of the results from NASA's Solar Maximum Mission*, K. T. Strong, J. L. R. Saba, B. M. Haisch and J. T. Schmelz, Eds. New York, Springer, vol. 143, 1999.

C. P. Liewer, M. Neugebauer and T. Zurbuchen, in *Solar Wind Ten*, M. Velli, R. Bruno and F. Malara, Eds. AIP Conf. Proc., vol. 679, Melville, NewYork, USA, 2003, p. 51.

J. A. Linker, Z. Mikic, P. Riley, R. Lionello and D. Odstrcil, in *Solar Wind Ten*, M. Velli, R. Bruno and F. Malara Eds. AIP Conf. Proc., vol. 679, Melville, NewYork, USA, 2003, p. 703.

D. J. McComas, H. A. Elliott, N. A. Schwadron, J. T. Gosling, R. M. Skoug and B. E. Goldstein, *Geophys. Res. Lett.* vol. 30, p. 1517, 2003.

D. J. McComas, J. T. Gosling and R. M. Skoug, *Geophys. Res. Lett.* vol. 27, p. 2437, 2000.

E. Marsch, Kinetic physics of the solar wind plasma, in *Physics of the Inner Heliosphere*, vol. 2, R. Schwenn and E. Marsch, Eds. Springer Verlag, Heidelberg, 1991, pp. 45-133.

E. Marsch and C. Y. Tu, *Solar Phys.* vol. 176, p. 87, 1997.

E. Marsch, W. I. Axford and J. F. McKenzie, "Solar Wind", in *Dynamic Sun* B.N. Dwivedi, Ed. Cambridge University Press, Cambridge, U.K., vol. 374, 2003.

E. Marsch, T. Wiegelmann and L. D. Xia, *Astron. Astrophys*., vol. 428, p.629, 2004.

E. Marsch, *Adv. Space Res*., in press, 2006.

N. R. Sheeley, Y. -M. Wang, S. H. Hawley et al., *Astrophys. J.*, vol. 484, p. 472, 1997.

T. Ohmi, M. Kojima, K. Hayashi et al., in *Solar Wind Ten*, M. Velli, R. Bruno and F. Malara, Eds. AIP Conf. Proc., vol. 679, Melville, NewYork, USA, p. 137, 2003.

R. Schwenn, A. Dal Lago, E. Huttunen and W. D. Gonzalez, *Ann. Geophys.* vol. 23, p. 1033, 2005.

R. Schwenn, "Solar wind sources and their variations over the solar cycle", *Space Sci. Rev*., in press, 2006.

C. J. Schrijver et al., *Nature*, vol. 394, p. 152, 1999.

N. Srivastava, R. Schwenn, B. Inhester, G. Stenborg and B. Podlipnik, *Space Sci. Rev.*, vol. 87, pp. 303-306, 1999.

N. Srivastava and R. Schwenn, in *The Outer Heliosphere: Beyond The Planets*, K. Scherer, H. Fichtner and E. Marsch, Eds. Copernicus Gesellschaft e.V., Katlenburg-Lindau, Germany, 2000, pp. 13-40.

O. C. St.Cyr, S. P. Plunkett, D. J. Michels et al., *J. Geophys. Res.*, vol. 105, p. 18169, 2004.

S. K. Solanki, M. Schüssler and B. Inhester, *Rep. Prog. Phys*., vol. 69, p. 563, 2006.

D. Tripathi, V. Bothmer and H. Cremades, *Astrophys. J.*, vol. 422, p. 337, 2004.

D. F. Webb and R. A. Howard, *J. Geophys. Res.*, vol. 99, p. 4201, 1994.

T. Wiegelmann and T. Neukirch, *Sol. Phys*., vol. 208, p. 233, 2002.

T. Wiegelmann and S. K. Solanki, Proc. the SOHO 15 Workshop - *Coronal Heating*, St. Andrews, Scotland, 6-9 September 2004, ESA SP 2004.

C. -Y. Tu, C. Zhou, E. Marsch, K. Wilhelm, L. Zhao, L.-D. Xia and J.-X. Wang, *Astrophys. J.*, vol. 624, L133, 2005b.

C. -Y. Tu, C. Zhou, E. Marsch, K. Wilhelm, L. -D. Xia, L. Zhao and J. -X. Wang, in *Solar Wind Eleven*, in press, 2006.

C. -Y. Tu, C. Zhou, E. Marsch, L. -D. Xia, L. Zhao, J. -X. Wang and K. Wilhelm, *Science*, vol. 308, p. 519, 2005a.

M. Zhang and B. C. Low, *Annual Rev. Astron. Astrophys.*, vol. 43, p. 103, 2005.